6th European Conference on Computational Mechanics (ECCM 6)
7th European Conference on Computational Fluid Dynamics (ECFD 7)
1115 June 2018, Glasgow, UK

TOPOLOGY OPTIMIZATION OF ELASTOMER DAMPING DEVICES FOR STRUCTURAL VIBRATION REDUCTION

S. Burri[1], A. Legay[1] and J-F. Deü[1]

[1]Laboratoire de Mécanique des Structures et des Systèmes Couplés (LMSSC),
Conservatoire national des arts et métiers (Cnam),
292 rue Saint-Martin 75003 Paris, France
{sylvain.burri, antoine.legay, jean-francois.deu}@lecnam.net[1]

Key words: Topology Optimization, rubber device

Abstract. Thanks to their damping properties, elastomer materials are commonly used in aeronautics and aerospace industry in order to manufacture damping devices, especially in terms of joints between sub-systems of mechanical assembling. In aeronautics, these damping joints can be used to protect electrical or optical on-board equipments from external noise and vibration sources. These joints should then deal with two contradictory aims: transmitting static loads and damping vibrations. The purpose of this work is to develop an efficient topology optimization tool for rubber devices.

1 INTRODUCTION

Thanks to their damping properties, elastomer materials are commonly used in aeronautics and aerospace industry in order to manufacture damping devices, especially in terms of joints between sub-systems of mechanical assembling. In aeronautics, these damping joints can be used to protect electrical or optical on-board equipments from external noise and vibration sources. These joints should then deal with two contradictory aims: transmitting static loads and damping vibrations. The purpose of this work is to develop a topology optimization tool for rubber devices. Two aspects should be considered:

- topology optimization based on a static criteria,
- topology optimization based on a dynamic criteria taking into account visco-elastic damping of the rubber device.

This paper concentrates on the first part: developing a topology optimization code considering a static criteria. In order to achieve this aim, a modified *Simple Isotropic Material with Penalization* (SIMP) method, with a static compliance criteria is firstly presented. Two different algorithms are then introduced: the *Optimality Criteria* (OC) method and the *Method of Moving Asymptotes* (MMA). An in-house finite element code is developed for any geometry (2D and 3D), any mesh, and for any boundary conditions

in terms of force and displacement. It is developed using the Python language for the global level and the Fortran language for the elemental level, while the meshes as well as the post-processing are done with Gmsh [8].

A validation case based on a literature benchmark (2D) is then computed and compared to the reference solution. Finally, a rubber device (3D) is optimized using a static criteria.

2 TOPOLOGY OPTIMIZATION USING A STATIC CRITERIA

Several optimization criteria can be chosen for a static mechanical problem depending on the targeted aim, such as for instance: mass, stress or displacement minimization. In this study, the minimization of the external forces work (compliance) is considered, under a final prescribed volume constraint. The compliance c and the volume constraint v are function of the material density distribution $\mathbf{x}$ and the purpose is to find the optimal set of $\mathbf{x} = [x_1, \ldots, x_n]^T$ that minimizes the compliance (n is the number of elements in the domain). The elemental Young's modulus E_i is, in the modified SIMP approach, written as follow:

$$E_i(x_i) = E_{\min} + x_i^p(E_0 - E_{\min}), \qquad x_i \in [0, 1] \tag{1}$$

where E_0 is the true stiffness of the material, $E_{\min}$ is chosen as non-zero so that to avoid singularity in the finite element stiffness matrix, and p is a penalization factor allowing to reach more easily $x_i = 1$ (presence of material) and $x_i = 0$ (void).

Furthermore, to avoid check-board patterns typical from SIMP method [1], a pseudo-density $\tilde{x}_i$ is introduced. It corresponds to the density of an element x_i ponderated by the elements densities in its neighbourhood N_i (including element i) and the factor $H_{ij} = r_{\min} - d_{ij}$ where d_{ij} is the distance between the centres of element i and an other element j in N_i, such that:

$$\tilde{x}_i = \frac{\sum_{j \in N_i} H_{ij} v_j x_j}{\sum_{j \in N_i} H_{ij} v_j} \tag{2}$$

where v_j is the volume of element j and $r_{\min}$ is an influence radius arbitrarily chosen by the user.

2.1 Simple Isotropic Material with Penalization method (SIMP)

Using Eq. (1) the global stiffness matrix can be expressed as follow:

$$\mathbf{K}(\tilde{\mathbf{x}}) = \sum_{i=1}^{n} \left[E_{\min} + \tilde{x}_i^p(E_0 - E_{\min})\right] \mathbf{K}_i^0 \tag{3}$$

where $\mathbf{K}_i^0$ is the global stiffness matrix corresponding to the assembly of the elemental stiffness matrices $\mathbf{k}_i^0$, themselves expressing the local stiffness with a unit Young's modulus.

The general optimization problem can be written as follow:

$$\begin{array}{rcc} \min\limits_{\tilde{\mathbf{x}}} & & c(\tilde{\mathbf{x}}) \\ \text{with} & : & c(\tilde{\mathbf{x}}) = \mathbf{U}(\tilde{\mathbf{x}})^T\mathbf{F} \\ \text{subject to} & : & v(\tilde{\mathbf{x}}) = \tilde{\mathbf{x}}^T\mathbf{v} - \alpha V_0 \leq 0 \\ & & \mathbf{0} \leq \tilde{\mathbf{x}}_\mathbf{i} \leq \mathbf{1} \\ & & \mathbf{K}(\tilde{\mathbf{x}})\mathbf{U}(\tilde{\mathbf{x}}) = \mathbf{F} \end{array} \tag{4}$$

where $\mathbf{v} = [v_1, \ldots, v_n]^T$ is the vector of elemental volumes, α the prescribed volume fraction, V_0 the initial volume of the domain, $\mathbf{U}(\tilde{\mathbf{x}})$ the nodal displacements vector and $\mathbf{F}$ the external nodal forces vector.

As in [3], the derivatives of the functions $c(\tilde{\mathbf{x}})$ and $v(\tilde{\mathbf{x}})$ are written as follow:

$$\frac{\partial c(\tilde{\mathbf{x}})}{\partial x_e} = \sum_{i \in N_e} \frac{\partial c(\tilde{\mathbf{x}})}{\partial \tilde{x}_i} \frac{\partial \tilde{x}_i}{\partial x_e} \tag{5}$$

$$\frac{\partial v(\tilde{\mathbf{x}})}{\partial x_e} = \sum_{i \in N_e} \frac{\partial v(\tilde{\mathbf{x}})}{\partial \tilde{x}_i} \frac{\partial \tilde{x}_i}{\partial x_e} \tag{6}$$

where $\frac{\partial \tilde{x}_i}{\partial x_e}$ can be deduced from Eq. (2):

$$\frac{\partial \tilde{x}_i}{\partial x_e} = \frac{H_{ie} v_e}{\sum_{j \in N_i} H_{ij} v_j} \tag{7}$$

It follows from the previous equations that the derivative of the compliance with respect to the pseudo-density $\tilde{x}_i$ is given by:

$$\frac{\partial c(\tilde{\mathbf{x}})}{\partial \tilde{x}_i} = -\mathbf{u}_i(\tilde{\mathbf{x}})^T \left[p\tilde{x}_i^{p-1}(E_0 - E_{\min})\mathbf{k}_i^0 \right] \mathbf{u}_i(\tilde{\mathbf{x}}), \tag{8}$$

where $\mathbf{u}_i(\tilde{\mathbf{x}})$ is the elemental displacement, while the derivative of the volume constraint with respect to the pseudo-density $\tilde{x}_i$ is given by:

$$\frac{\partial v(\tilde{\mathbf{x}})}{\partial \tilde{x}_i} = v_i \tag{9}$$

2.2 Optimality Criteria method (OC)

A common numerical algorithm for optimum reaching is the standard optimality criteria (OC) method (Bendsøe, 1995). This method is based on Lagrange multipliers which can be written from the objective $c(\tilde{\mathbf{x}})$ and constraint $v(\tilde{\mathbf{x}})$ functions:

$$\mathfrak{L} = c(\tilde{\mathbf{x}}) + \lambda v(\tilde{\mathbf{x}}) \tag{10}$$

where λ denotes the Lagrange multiplier associated with the volume constraint. It is important to note that the "+" sign is due to constraint's convexity. The minimization

is reached when the derivatives of the Lagrangian with respect to $\tilde{x}_e$ and with respect to the Lagrange multiplier λ are equal to zero:

$$\frac{\partial \mathfrak{L}}{\partial x_e} = \frac{\partial c(\tilde{\mathbf{x}})}{\partial x_e} + \lambda \frac{\partial v(\tilde{\mathbf{x}})}{\partial x_e} = 0 \tag{11}$$

$$\frac{\partial \mathfrak{L}}{\partial \lambda} = \tilde{\mathbf{x}}^T \mathbf{v} - \alpha V_0 = 0 \tag{12}$$

From Eq. (11), the optimality condition $B_e = 1$ [4], can be deduced:

$$\forall e \in [1, \cdots, n] \quad B_e = \frac{-\frac{\partial c(\tilde{\mathbf{x}})}{\partial x_e}}{\lambda \frac{\partial v(\tilde{\mathbf{x}})}{\partial x_e}} \tag{13}$$

For each step and each design variable x_e, $\frac{\partial c(\tilde{\mathbf{x}})}{\partial x_e}$ and $\frac{\partial v(\tilde{\mathbf{x}})}{\partial x_e}$ are known. A dichotomy algorithm is then used in order to find λ such that $B_e = 1$. As soon as $B_e = 1$, the set of $\tilde{\mathbf{x}}$ may be the optimal solution if the prescribed volume is ensured.

It is important to notice that, considering Eq. (8) and Eq. (9), $\frac{\partial c(\tilde{\mathbf{x}})}{\partial x_e}$ is always negative in static, but not in dynamic using the dynamic compliance formulation described in [4]. As $\frac{\partial v(\tilde{\mathbf{x}})}{\partial x_e}$ is always positive, B_e is always positive through the iterative process ($\lambda \geq 0$ by definition). OC is then well designed to solve static compliance problems but not for a dynamic compliance problems because B_e can be negative.

The update of the new variable x_e follows the original paper (Sigmund, 2001):

$$x_e^{k+1} = \begin{cases} \max(0, x_e - m) & \text{if } x_e B_e^{\eta} \leq \max(0, x_e - m), \\ \min(1, x_e + m) & \text{if } x_e B_e^{\eta} \geq \min(1, x_e + m), \\ x_e^k B_e^{\eta} & \text{otherwise,} \end{cases} \tag{14}$$

where k is the k^{th}-iteration, m is a positive move-limit restraining the speed of the convergence so that to stay in the admissible domain and η ($= 1/2$) is a numerical damping. The optimum solution is reached when $x_e^{k+1} - x_e^k$ is less than a chosen small value.

2.3 Method of Moving Asymptotes (MMA)

Since OC is not able to deal with dynamic optimization problems, another numerical algorithm has to be used. The chosen one in this work is the method of moving asymptotes (MMA) introduced by Svanberg [5].

MMA uses convex approximation functions [6] in order to represent, in each iteration, the true functions of the problem. Two approximations $\tilde{f}_c^k(\tilde{\mathbf{x}})$ and $\tilde{f}_v^k(\tilde{\mathbf{x}})$ are generated, respectively based on $c(\tilde{\mathbf{x}})$ and $v(\tilde{\mathbf{x}})$, such as:

$$\tilde{f}_g^k(\tilde{\mathbf{x}}) = g^k(\tilde{\mathbf{x}}) - r^k = \sum_{i=1}^{n} \left(\frac{p_i^k}{u_i^k - \tilde{x}_i} + \frac{q_i^k}{\tilde{x}_i - l_i^k} \right) \tag{15}$$

where $g = \{c, v\}$, r^k is a residual resulting from the difference between $\tilde{f}_g^k(\tilde{\mathbf{x}})$ and $g^k(\tilde{\mathbf{x}})$, u_i^k and l_i^k are the so-called *moving asymptotes* which vary in each iteration according to

x_i, and finally p_i^k and q_i^k are respectively functions of $\frac{\partial g(\tilde{\mathbf{x}})}{\partial x_e} > 0$ and $\frac{\partial g(\tilde{\mathbf{x}})}{\partial x_e} < 0$. Thus, MMA is not impacted by the sign of $\frac{\partial g(\tilde{\mathbf{x}})}{\partial x_e}$ and can properly be used in the dynamic case.

As OC criteria, MMA is also a dual method using Lagrange multipliers. However, the considered Lagrangian takes into account the design variables bounds α and β which are restrictions of typical bounds of x_i (0 and 1) in order to increase the robustness during the convergence process:

$$\mathfrak{L} = \tilde{f}_c^k(\tilde{\mathbf{x}}) + \lambda(\tilde{f}_v^k(\tilde{\mathbf{x}}) + r^k) + \sum_{i=1}^{n} \Big[\xi(x_i - \alpha) + \eta(\beta - x_i)\Big] \tag{16}$$

Derivating Eq. (16) by the inner variables ($\tilde{\mathbf{x}}$, λ, ξ, η) and relaxing the optimality conditions, a Newton scheme as below is used to compute the next iteration:

$$\omega^{\ell+1} = \omega^{\ell} + \tau \cdot \Delta\omega^{\ell} \tag{17}$$

where $\omega^{\ell} = (x^{\ell}, \lambda^{\ell}, \xi^{\ell}, \eta^{\ell})$ and $\Delta\omega^{\ell} = (\Delta x^{\ell}, \Delta\lambda^{\ell}, \Delta\xi^{\ell}, \Delta\eta^{\ell})$. More details about the full algorithm are available in Svanberg's papers (Svanberg, 1987 & 2007).

3 VALIDATION AND APPLICATIONS

3.1 Validation

In order to validate the implementation of the OC and MMA methods in our in-house code, a test-case taken from [2] is solved. This problem, named the MBB beam, is described in Fig. 1. As in [2], the mesh is composed of 60×20 4-nodes quadrangle elements, the penalty factor p is taken to 3, the neighbourhood is defined with $r_{\min} = 2.4$ and the final prescribed volume fraction is equal to 50% of the initial volume domain.

The final obtained shape (Fig. 2) is very similar to the one presented in [2]. Moreover, when comparing the global compliance values for the OC method, both are almost equivalent: 216.81 for [2], 216.60 with the house code. The MMA method gives a similar optimized shape (Fig. 2) and a slightly different compliance, equals to 218.15.

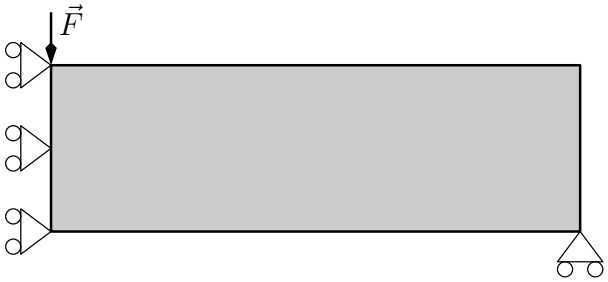

Figure 1: 2D MBB beam - Design domain, including boundary conditions

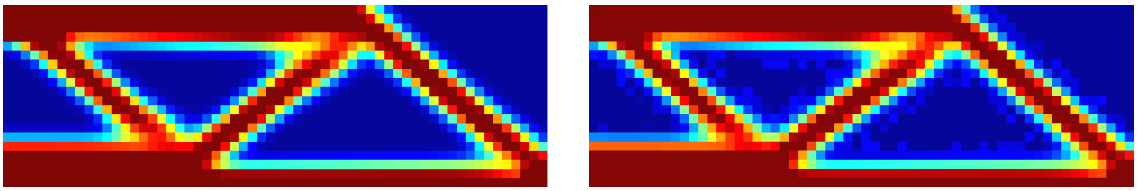

Figure 2: 2D MBB beam - Optimized topology of the beam - Left: OC method - Right: MMA method (red: $x_e = 1$, blue: $x_e = 0$)

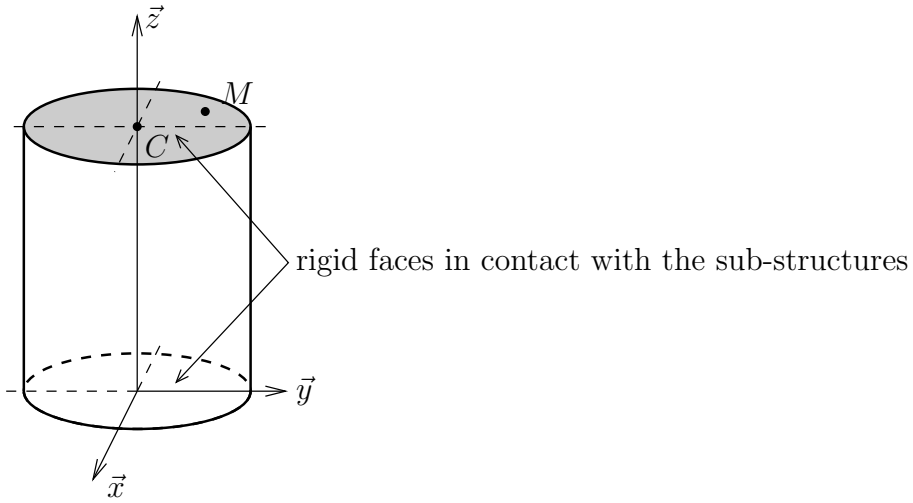

Figure 3: Initial design domain of the rubber device

3.2 Application to a rubber device

3.2.1 Presentation

The proposed application is the topology optimization of a device used to dissipate the transmitted vibrations between two sub-structures. A complete dynamical study of a system made of a structure supported by four devices can be found in [7]. In this present work, as a first step, the optimization of the device is done using a static compliance criteria.

The design domain as well as the two faces of the device in contact with the two different sub-structures are presented on Fig. 3. Since the device is in contact with much more rigid materials (typically metal) than its constitutive material (typically rubber), the upper and lower faces are considered as rigid bodies. Thus, each face has 6 degrees of freedom (3 translations and 3 rotations), and each node M of a face is linked to these 6 dofs:

$$\overrightarrow{u}_M = \overrightarrow{u}_C + \overrightarrow{MC} \wedge \overrightarrow{\Omega} \tag{18}$$

where $\overrightarrow{u}_M$ is the displacement of the node M, C is the centre of the face, $\overrightarrow{u}_C$ is the displacement of the centre of the face (3 translations) and $\overrightarrow{\Omega}$ corresponds to the rotation

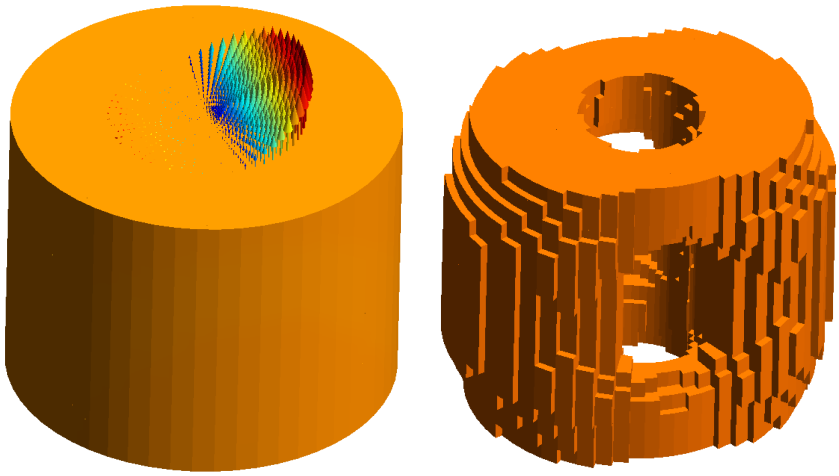

Figure 4: Topology optimization of the rubber device for a bending load - Design domain (left) and final solution (right)

of the interface (3 rotations). This relation allows to write any displacement of an interface point M as the product between a transfer matrix and an augmented vector of the interface centre dofs in an orthonormal system of coordinates $(\vec{x}, \vec{y}, \vec{z})$:

$$\begin{bmatrix} u_M \\ v_M \\ w_M \end{bmatrix} = \begin{bmatrix} 1 & 0 & 0 & 0 & (z_M - z_C) & (y_C - y_M) \\ 0 & 1 & 0 & (z_C - z_M) & 0 & (x_M - x_C) \\ 0 & 0 & 1 & (y_M - y_C) & (x_C - x_M) & 0 \end{bmatrix} \begin{bmatrix} u_C \\ v_C \\ w_C \\ \Omega_x \\ \Omega_y \\ \Omega_z \end{bmatrix}, \tag{19}$$

where (x_M, y_M, z_M) and (x_C, y_C, z_C) are the coordinates of points M and C, (u_M, v_M, w_M) and (u_C, v_C, w_C) are the displacements of points M and C and $(\Omega_x, \Omega_y, \Omega_z)$ are the interface rotation components. All interface node's dofs are then eliminated from the global finite element model.

The material properties of the rubber device are given by:

- Young modulus E= 0.5 MPa
- Poisson's coefficient $\nu = 0.45$

Finally, the mesh is composed of 33,516 8-nodes hexahedral elements, the chosen penalty factor p is 3, the neighbourhood is defined with a $r_{\min}$ calculated for each element such that about 10 to 30 elements are in the neighbourhood of the considered element. The final prescribed volume fraction is equal to 0.4.

3.2.2 Results and discussion

The first case is a bending load: the lower face is fixed and a torque along the transverse axis $\vec{x}$ of the device is applied on the upper face. Figure 4 both shows the design domain

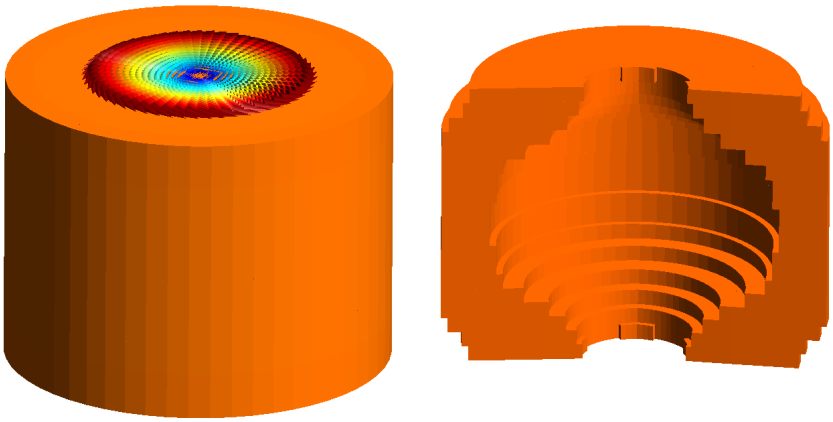

Figure 5: Topology optimization of the rubber device for a torsion load - Design domain (left) and final solution (right)

with the load and the final optimized shape. The final solution has two different holes. The one on the longitudinal axis $\vec{z}$ is due to the fact that faces are stiffen. The second one, on the transverse axis $\vec{x}$, is due to bending solicitation: the stress is more important on the extremities (where material is present) than in the middle (where material is removed).

The second case is a torsion load: the lower face is fixed, and a torque along the axis $\vec{z}$ of the device is applied on the upper face. Figure 5 both shows the design domain with the load and the final optimized shape. The final solution has a longitudinal hole due to the fact that the stress is more important at the external skin of the cylinder than in the middle. The hole is wider in the middle of the device, due to the rigid faces assumption.

4 Conclusion and ongoing work

This work concerns the topology optimization of elastomer damping devices. The OC and MMA methods have been implemented. The validation case for a static compliance criteria shows that the implementation has been done correctly. As a first step in the more global vision of the project, a damping device is optimized in this work with a static compliance criteria. An ongoing work on vibration damping is performed using a fractional derivative Zener model of the elastomer [9] and a dynamic compliance [10, 11].

Acknowledgements

The support of ArianeGroup as well as the courtesy of Svanberg are gratefully acknowledged.

REFERENCES

[1] O. Sigmund, A 99 line topology optimization code written in Matlab, *Structural and Multidisciplinary Optimization* (2001) **21**:120–127

[2] E. Andreassen, A. Clausen, M. Schevenels, B. Lazarov, and O. Sigmund, Efficient topology optimization in MATLAB using 88 lines of code, *Structural and Multidis-*

ciplinary Optimization (2011) **43**:1–16

[3] K. Liu, A. tovar, An efficient 3D topology optimization code written in Matlab, *Structural and Multidisciplinary Optimization* (2014) **50**:1175–1196

[4] M. Bendsoe, O. Sigmund, Topology optimization – Theory, Methods, and Applications, Springer, Berlin Heidelberg New York (2004)

[5] K. Svanberg, MMA and GCMMA - two methods for nonlinear optimization, available on *https://people.kth.se/∼krille/mmagcmma.pdf*

[6] P. Duysinx, M. Bruyneel, C. Fleury Solution of topology optimization problems with sequential convex programming available on *https://orbi.uliege.be/bitstream/2268/100151/1/OA56.pdf*

[7] B. Morin, A. Legay and J.-F. Deü, Reduced order models for dynamic behavior of elastomer damping devices, *Finite Elements in Analysis and Design* (2018) **143**:66–75

[8] C. Geuzaine and J.-F. Remacle, Gmsh: A 3-D finite element mesh generator with built-in pre- and post-processing facilities, *International Journal for Numerical Methods in Engineering* (2009) **79**:1309–1331

[9] A. C. Galucio, J.-F. Deü, R. Ohayon, Finite element formulation of viscoelastic sandwich beams using fractional derivative operators, *Computational Mechanics* (2004) **33**:282–291

[10] A. Takezawa, M. Daifuku, Y. Nakano, K. Nakagawa, T. Yamamoto, M. Kitamura, Topology optimization of damping material for reducing resonance response based on complex dynamic compliance, *Journal of Sound and Vibration* (2016) **365**:230–243

[11] W.-S. Lee, S.-K. Youn, Topology optimization of rubber isolators considering static and dynamic behaviours, *Structural and Multidisciplinary Optimization* (2004) **27**:284–294